PHYSICAL REVIEW D **77,** 063511 (2008)

Cosmological avatars of the landscape. II. CMB and LSS signatures

R. Holman*
Department of Physics, Carnegie Mellon University, Pittsburgh, Pennsylvania 15213, USA

L. Mersini-Houghton†
Department of Physics and Astronomy, UNC-Chapel Hill, North Carolina 27599-3255, USA

T. Takahashi‡
Department of Physics, Saga University, Saga 840-8502, Japan
(Received 19 December 2006; published 6 March 2008)

This is the second paper in the series that confronts predictions of a model of the landscape with cosmological observations. We show here how the modifications of the Friedmann equation due to the decohering effects of long wavelength modes on the wave function of the Universe defined on the landscape leave unique signatures on the CMB spectra and large scale structure (LSS). We show that the effect of the string corrections is to suppress σ_8 and the CMB temperature-temperature (TT) spectrum at large angles, thereby bringing WMAP and SDSS data for σ_8 into agreement. We find interesting features imprinted on the matter power spectrum $P(k)$: power is suppressed at large scales indicating the possibility of primordial voids competing with the integrated Sachs-Wolfe effect. Furthermore, power is enhanced at structure and substructure scales, $k \simeq 10^{-2-0}h$ Mpc^{-1}. Our smoking gun for discriminating this proposal from others with similar CMB and LSS predictions comes from correlations between cosmic shear and temperature anisotropies, which here indicate a noninflationary channel of contribution to LSS, with unique ringing features of nonlocal entanglement displayed at structure and substructure scales.

DOI: 10.1103/PhysRevD.77.063511 PACS numbers: 98.80.Qc, 11.25.Wx

I. INTRODUCTION

While finding a dynamical reason for why certain initial conditions for the Universe were preferred over others would be a major step forward in our understanding of nature, such a proposal must also be falsifiable. In previous work [1,2], we have argued that the quantum dynamics of gravity acting on the string landscape, treated as the configuration space of initial conditions [3,4], could in fact show why the initial conditions for high scale inflation are natural.

In the previous paper of this series (hereafter referred to as paper I) [5], we showed how tracing out long wavelength modes of metric and matter field fluctuations could decohere the wave function of the Universe, defined on this configuration space. This results in both inducing a highly nonlocal entanglement between our horizon patch with others as well as giving rise to corrections to the Friedmann equation. We then used these cosmological effects to bracket the scale of SUSY breaking b which appears as one of the parameters determining the size of the nonlocality of entanglement. The SUSY breaking bounds were derived by requiring that constraints on the flatness of the modified inflaton potential and the amount of density perturbations be satisfied when the quantum gravity corrections are taken into account.

The backreaction effects that modify the Friedmann equations during inflation (essentially correcting the potential) will also modify the power spectrum. These modifications affect a number of cosmological observables, such as the CMB temperature anisotropy [the temperature-temperature (TT) spectrum], large scale structure (LSS), the creation and statistics of voids, as well as running of the scalar spectral index n_s. We discuss these in detail in Sec. III. In particular, we find a natural explanation for the disagreement between SDSS and WMAP data on the low value of σ_8 and for the observed low l anomaly in the CMB (temperature anisotropies) TT-spectrum observed both by COBE [6] as well as by WMAP [7]. We then turn to a discussion of how the backreaction effects may contribute with a negative density contrast that gives rise to the creation of primordial voids in Sec. III. We also show how the effects we find here can be distinguished from other effects predicted by other models of quantum gravity. The main tool we use to do this is the cross correlation $C_{l,TL}$ of temperature (T) with the lensing potential of cosmic shear (L).

We collect all of our results and discuss their regimes of validity in Sec. IV, and then conclude.

II. QUANTUM EFFECTS OF THE LANDSCAPE

For completeness, we recall some of the basic relations found in paper I. As in paper I, we follow Ref. [8] and use the following inflaton potential, (see also [9]):

*rh4a@andrew.cmu.edu
†mersini@physics.unc.edu
‡tomot@cc.saga-u.ac.jp

$$V(\phi) = V_0 \exp\left(-\lambda \frac{\phi}{M_{\rm P}}\right). \quad (2.1)$$

While this potential can appear in supergravity based models of inflation, we use it more for illustrative purposes, due to its simplicity. Our results will hold generically for any single field inflaton potential that satisfies the slow-roll conditions.

After including the backreaction due to the long wavelength modes being traced out, the right-hand side of the effective Friedmann equation was shown to be modified as [5]

$$H^2 = \frac{1}{3M_{\rm P}^2}\left[V(\phi) + \frac{1}{2}\left(\frac{V(\phi)}{3M_{\rm P}^2}\right)^2 F(b, V) \right] \equiv \frac{V_{\rm eff}}{3M_{\rm P}^2}, \quad (2.2)$$

where

$$F(b, V) = \frac{3}{2}\left(2 + \frac{m^2 M_{\rm P}^2}{V}\right)\log\left(\frac{b^2 M_{\rm P}^2}{V}\right) - \frac{1}{2}\left(1 + \frac{m^2}{b^2}\right)\exp\left(-3\frac{b^2 M_{\rm P}^2}{V}\right). \quad (2.3)$$

We have taken $8\pi G_N = M_{\rm P}^{-2}$ and the scale of the nonlocal entanglement is given by the interference length L_1, derived in [5]:

$$L_1^2 = \frac{a}{H}\left[\left(\frac{m^2}{3H} + H\right)\ln\frac{b}{H} - \frac{m^2 H}{6}\left(\frac{1}{b^2} - \frac{1}{H^2}\right)\right]. \quad (2.4)$$

The primordial power spectrum is estimated from

$$P_{\mathcal{R}} = \frac{1}{75\pi^2 M_{\rm P}^2}\frac{V_{\rm eff}^3}{V_{\rm eff}'^2}. \quad (2.5)$$

For the initial potential, given in Eq. (2.1), we have

$$P_{\mathcal{R}}^0 = \frac{1}{75\pi^2 M_{\rm P}^2}\frac{V_0}{\lambda^2 M_{\rm P}^4}. \quad (2.6)$$

The scalar spectral index before modifications is given by $n_s^0 - 1 = -\lambda^2$. Modifications in the Friedmann equation result in a running of the spectral index $n_s = n_s^0 + \delta n_s$, as we describe below.

The solution for the inflaton field in the presence of the corrected potential is given by

$$\phi = \lambda M_{\rm pl}\left[1 + \frac{1}{2}\frac{1}{3M_{\rm pl}^2}\left(\frac{V_0}{3M_{\rm pl}^2}\right)\left\{3\left(2 + \frac{m^2 M_{\rm pl}^2}{V_0}\right) \times \log\left(b\sqrt{\frac{3M_{\rm pl}}{V_0}}\right) - \frac{1}{2}\left(1 + \frac{m^2}{b^2}\right)e^{-3M_{\rm pl}^2 b^2/V_0}\right\}\right]^{-1} \times \log\left(\frac{k}{k_{\rm ref}}\right), \quad (2.7)$$

where $k_{\rm ref} \simeq (4000\ {\rm Mpc})^{-1}$.

Define $3M_p^2/F(b, V) \equiv \sigma(b, \phi)$ and denote the energy correction $V^2/\sigma = f(b, V)$. The modified Friedmann equation can then be written as

$$3M_p^2 H^2 = V + f(b, V). \quad (2.8)$$

An important fact is that $f(b, V)$ is a negative function, so that the new Friedmann equation only makes sense in the regime where $V + f(b, V) > 0$.

We are now prepared to examine the effects of this modification on large scale structure and the CMB.

III. SIGNATURES OF THE LANDSCAPE ON CMB AND LSS

Armed with our modified Friedmann equation and power spectrum, we are now ready to compute the corrections to the CMB power spectrum and to large scale structure (LSS).

In Fig. 1 we show the results obtained using CMBFAST [10] with the modification in the primordial spectrum of Eq. (2.2) for $b \simeq 10^{-9} M_{\rm P}$. For comparison, we also plot the case with ΛCDM and data from WMAP3 [7]. For the plot, we fixed the parameters for the inflaton potential as $\lambda = 0.1$ and $V_0 = 8.0 \times 10^{-8} M_{\rm P}^4$ and $1.0 \times 10^{-8} M_{\rm P}^4$ for $b = 4.0 \times 10^8$ GeV and 3.8×10^9 GeV, respectively. The cosmological parameters are taken to be $\Omega_m h^2 = 0.12$, $\Omega_b h^2 = 0.023$, $h = 79$, $\tau = 0.091$, and $n_s = 0.99$ for Lambda cold dark matter (LCDM) models. For the cases with our model, we varied them slightly to fit the spectrum to WMAP3 data around the acoustic peaks.

It can be seen from Fig. 1 that power at low l is suppressed compared to the concordance LCDM model.

Consistency with the Einstein equations in deriving the primordial spectrum requires that we include the pressure corrections corresponding to the energy modification equation (2.2). This correction directly contributes to the velocity of the inflaton field $\dot{\phi}$ and therefore to the running of the scalar index n_s as discussed further below. The pressure contribution from the correction term for the inflaton with energy density $\rho \approx V$ is

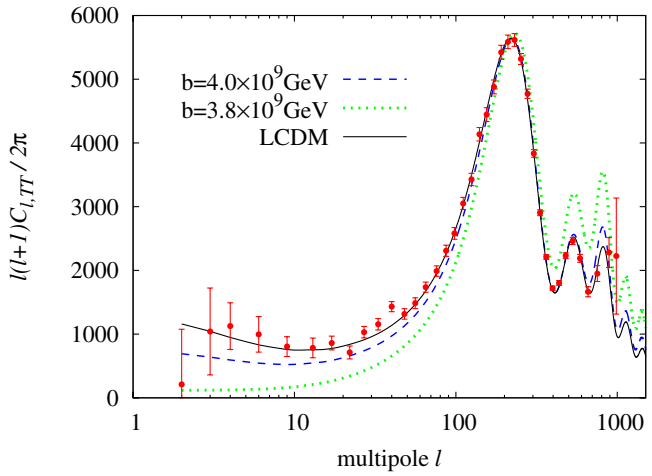

FIG. 1 (color online). CMB TT power spectra for the cases with $b = 4.0 \times 10^9$ GeV (dashed line) and 3.8×10^9 GeV (dotted line). For reference, the spectrum for the ΛCDM case (solid line) and the data from WMAP3 are also plotted.

$$p_f = (\rho + p)\frac{df(b,V)}{d\rho} - f(b,V). \tag{3.1}$$

Including this modification into the expression for the primordial spectrum and replacing the field solutions, Eq. (2.7), in $P_{\mathcal{R}}$ in order to obtain $P_{\mathcal{R}}$ as a function of the wave number k, we get

$$P_{\mathcal{R}} = \frac{1}{75\pi^2 M_{\rm P}^2}\frac{V_0(1+V_0/2\sigma)^3}{\lambda^2 M_{\rm P}^4} g(b,\phi) \simeq \left(\frac{k}{k_{\rm ref}}\right)^{n_s-1}, \tag{3.2}$$

where

$$g(b,\phi) = \left(1 + 4\pi\left(\frac{f(b,V)+p_f}{M_P^2\dot{H}}\right)\right)^{-2} \simeq \left(\frac{k}{k_{\rm ref}}\right)^{\delta n_s}. \tag{3.3}$$

For the parameter choice described above, the maximum power is roughly on scale 180 Mpc. The modified $P_{\mathcal{R}}$ is an increasing function of k for small scales and a decreasing function at large scales. This gives rise to a suppression of power on quadrupole scales and a running of the spectral index n_s. The spectrum tilts a little to the blue on large scales and has a slight running towards red in small scales for some parameter sets. This feature can be seen in Fig. 1, in particular, for the case with $b = 4.0 \times 10^9$ GeV. Now let us look at these effects in more detail.

A. Suppressed σ_8

As seen from the figure, the suppression around the quadrupole results in a 30% decrease on the rms amplitude σ_8. This is a direct result of the modification of the Newtonian potential $\delta\Phi$ by the *negative* modification term $f(b,V)$ on quadrupole scales. From the Poisson equation the Newtonian potential is given by $-2/3(kaH)^2\Phi = 4\pi G_n\rho$. The correction to the gravitational potential is of second order and comes from the addition of the non-Gaussian perturbation $f(b,V)$ to the adiabatic Gaussian perturbations V: $\nabla^2\delta\Phi = 4\pi G_N f(b,V)$, where

$$\Phi = \Phi^0 + \delta\Phi \simeq \Phi^0\left[1 + \frac{f(b,V)}{\rho}\left(\frac{r}{L_1(k,b)}\right)^2\right]. \tag{3.4}$$

The largest contribution to the Newtonian potential from the modification in the primordial spectrum, Eqs. (3.2) and (3.3), is at $k \simeq 1$ corresponding to present-day scales of $\simeq 10^{-4}$ Mpc, i.e. at the quadrupole level. The induced correction to the quadrupole, calculated in I to be

$$\begin{aligned}(\nabla T/T)_{\rm quad} &\approx r_H^2\nabla^2\delta\phi = (ck_1/H_0)^2\delta\phi \\ &\approx 0.5(r_H/L_1)^2(\delta\rho/\rho)_1,\end{aligned} \tag{3.5}$$

originates from the inhomogeneities superimposed on the background potential at scales L_1 which is at least 100 to 1000 times the size of the horizon. Note that $\delta_f \equiv (\delta\rho/\rho)_1 \simeq f(b,V)/V$ is negative. Therefore the corrected potential contributes a negative density contrast δ_f which is superimposed on the positive Gaussian density perturbations. This results in a lowering of the amplitude σ_8 by around 20%–30%. It is very interesting that, due to the tight bounds on b found in paper I, the amplitude suppression is forced to be 20%–30% less than the amplitude in a LCDM cosmology. This then brings the WMAP results for $\sigma_8 \simeq 1.1$ in agreement with the 2DF and SDSS findings [11] $\sigma_8 \simeq 0.8$.

Another interesting fact that we will comment on further below is that the negative density correction results in a void being generated around $k \simeq 1$.

B. Running of the scalar spectral index, δn_s

The running of the spectral index $\delta n_s = n_s - n_s^0$ can be readily estimated from Eqs. (3.2) and (3.3) above. Since the modified spectrum is $P_{\mathcal{R}} \simeq (k/k_{\rm ref})^{n_s-1}$ and the unmodified power spectrum $P^0_{\mathcal{R}} \simeq (k/k_{\rm ref})^{n_s^0-1}$, it follows that

$$\delta n_s = \frac{d\ln g(b,\phi)}{d\ln k} = \frac{\dot{\phi}}{H}\left(\frac{d\ln g(b,V)}{d\phi}\right). \tag{3.6}$$

Corrections to the potential are very small. Besides, in paper I we imposed the condition that $V_{\rm eff}$ must continue to satisfy the slow-roll conditions, which led us to an upper bound for the SUSY breaking parameter b. Therefore the kinetic term $\dot{\phi}^2$ is small even with the correction included in the potential. The running of the spectral index $\delta n_s(k)$ as a function of k can now be estimated by replacing $\dot{\phi} \approx -V'_{\rm eff}/3H$ and using the solution for ϕ in Eq. (2.7). The expression is very long and not particularly illuminating so instead of writing it here we can just describe the relevant features. The maximum running is at low wave numbers, the result of which is a suppression of the TT-spectrum at low multipoles, Fig. 1. The reason for this is that the correction term in the Friedmann equation has its maximum effect at the onset of inflation when $V \simeq \sigma(b,V)$, and therefore the inflaton slow roll is disturbed near the scales corresponding to the first few e-foldings. This results in suppressed power at these scales. As V decreases during inflation the correction term is redshifted away. The overall running tends towards the blue at low multipoles and towards the red at higher multipoles.

Unlike the models in Refs. [8,12], the correction terms that modify the Friedmann equation, and therefore the energy and length cutoff scales $\sigma(b,V,L_1(b,V))$ in our model, are dynamical. By this we mean that their scale of influence changes with k since due to the interlocking of b and V contained in $\sigma(b,V)$, the ratio $b^2/V(\phi)$ changes as ϕ rolls down its potential. This results in three different regimes for the slow-roll of inflaton and generation of perturbations. At the onset of inflation, the two energy terms in H^2 are comparable, thus the amplitude of perturbations and TT power is suppressed around the quadrupole. The dominant contribution in the interference length

comes from the exponential term, which as we mentioned before, arises from tunneling to and from other patches.

When k_{18}[1] leaves the horizon, the inflaton potential V/M_P^2 becomes comparable to b^2 and thus the exponential in the correction term dominates over the logarithmic term. This results in a discontinuity of δn_s around k_{20} which suppresses the perturbations of $k \simeq 18$–20, corresponding to the scale 140–180 Mpc today. This discontinuity is important for structure formation features as discussed below.

A second discontinuity occurs around k_{40} towards the end of inflation where V has dropped so much that the exponential term in $\sigma(b, V)$ is nearly zero and the energy correction is dominated by the log term. Furthermore, as V drops below b^2, the log term and $f(b, V)$ change sign from negative to positive energy corrections, which creates a jump discontinuity at $k \simeq 40$ for n_s and thus another suppressed perturbation around a scale which at present is deep into the scales relevant for substructure formation.

C. LSS, voids, and the axis of evil

We described above the effect of the dynamic modification term on the background potential. Until $k = 40$, this modification is negative and the correction to Φ lowers structure there. Thus, we have a perturbation channel originating from the entanglement modification term which produces inhomogeneous, non-Gaussian, and non-adiabatic anisotropies $\delta\Phi/\Phi^0$ that are superimposed on the Gaussian perturbations generated by the inflaton potential V [cf. Eq. (3.4)].

The present-day Newtonian background potential can be estimated from Eq. (3.4) through the expression $\Phi(r, z) = (1 + z)G(z)\Phi(r, 0)$, where $G(z)$ is the growth factor of structure and r, z are the physical comoving distances and redshifts, respectively. It should be noted that the correction term here is scale dependent since it involves a coupling of the b, V channels for the highly nonlocal entanglement with size $L_1 \gg r_H$. Since most of the matter in our universe is made of dark matter, we can view the above modification to the background Newtonian potential as a perturbation on dark matter, denoted by $(\delta\rho/\rho)_1$ in the previous section, but of arising due to quantum entanglement, as opposed to having an inflationary origin.

In Fig. 2, we plot the matter power spectrum calculated with the modifications in our model. For comparison we also plot the results of the LCDM model as well as the SDSS data [11]. Here the parameters for the inflaton potential are taken as $\lambda = 0.1$ and $V_0 = 8.0 \times 10^{-8} M_{\rm P}^4$. We varied the overall normalization slightly to fit the data by using the uncertainty of the bias.

As can be seen from Fig. 2 for the matter power spectrum $P(k)$, the negative contribution from the modification

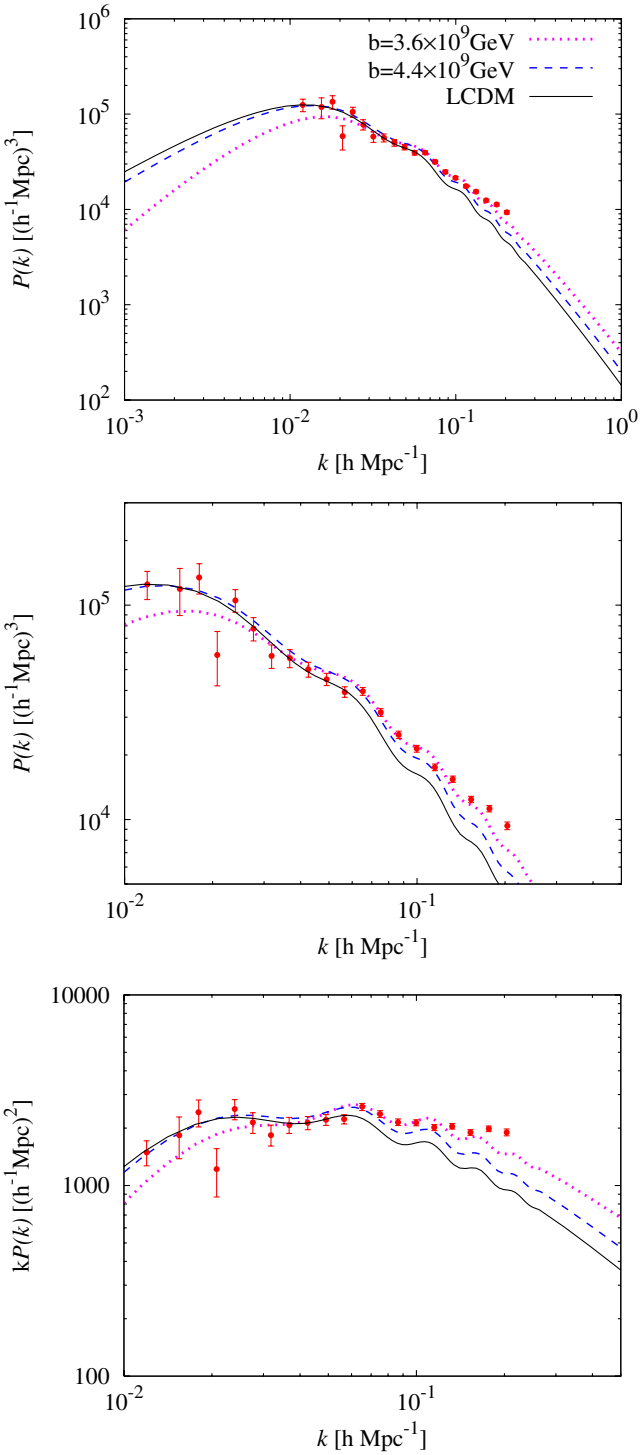

FIG. 2 (color online). Matter power spectra for the same values of b as Fig. 1, described in Sec. III. For comparison, the case with ΛCDM (solid line) and the data from SDSS are also plotted. The top panel shows $P(k)$ for several orders of k, the middle panel is the same as the top panel except the range of k to look at the scales seen by SDSS, and the bottom panel shows $kP(k)$.

of the energy density during inflation, which takes its maximum value at large scales, results in less structure at very large scales in our model compared to the concord-

[1]Here the notation k_{18} means that the scale which exits the horizon 18 e-folds after the onset of inflation.

ance cosmology LCDM. This is due to the negative correction in Eq. (3.4) which gives rise to a negative density contrast denoted above by $\delta_f < 0$ being superimposed on the positive background potential thereby resulting in damped structure formation and the creation of primordial voids at those large scales. We discussed above how the correction to the quadrupole amplitude which damps power on these scales also produces the first void at around $k \simeq 1$, when evolved to present times, resulting also in a compensation of the integrated Sachs-Wolfe effect of dark energy. This void is unaffected by the nonlinear physics of the subsequent structure growth since it is located at low multipoles where the potential is nearly constant. According to Inoue and Silk [13], a void-induced quadrupole of any size can explain the two cold spots observed by SDSS [11] in the sky at $(\Delta T/T)_{\rm quad} < 0$ and the alignment of quadrupole with octupole along the preferred axis which here is the direction that joins the two voids at 60 degrees on the sky, namely, the axis of evil. We refer the reader to Ref. [13] for the details of this calculation.

We expect the second void to form at the first discontinuity in the kinetic term $\dot{\phi}$, $V'_{\rm eff}$ corresponding to scales $k = 20$ or about 200 Mpc at redshifts about $z \sim 1$. This void would correspond to an angle less than a degree in the sky today, which may be related to the unusual cold spot observed in the southern hemisphere, as discussed in Ref. [13]. However, a deeper understanding of this point requires dealing with the nonlinear growth of structure at these scales. It is unclear to us whether these structures will persist after nonlinear evolution to the present epoch.

Although the second discontinuity would suppress the background perturbations at around $k = 40$, it would not produce voids now the superimposed nonadiabiatic perturbation from the modification term has a positive density contrast, which serves to enhance structure formation rather than suppress it (Fig. 2).

Figure 2, confirms that power is indeed suppressed compared to LCDM at large scales. However, unlike in the LCDM situation, it is enhanced at structure and substructure scales. As far as the linear theory is concerned, $P(k)$ in our model is in closer agreement with the SDSS data than the conventional LCDM model. For $k < 0.09\ h/\mathrm{Mpc}$, nonlinear evolution can alter the matter power spectrum. Thus, our model may have implications for the nonlinear evolution of structure. We would like to emphasize here that we have no room to change the parameters b, V in order to fit the data shown in Fig. 2 since the effect is derived from a highly nontrivial and nonlocal term that couples b, V.

D. Cosmic shear and its correlation with temperature anisotropies, $C_{l,TL}$

How can we distinguish our model from other models that might predict suppression of power at low l? This crucial issue was addressed in [14] with the result that the best tool to use to discriminate between models is the prediction for the cross correlation between the TT and the cosmic shear LL lensing potential which traces out the large scale structure of the universe. Doing this gives us a direct comparison between the sources that seed both types of perturbations. The standard picture of the generation of fluctuations in inflationary cosmologies provides only one source, the primordial spectrum, for seeding both CMB and LSS and therefore predicts a correlation of order one on large scales. On the other hand, models with input from quantum gravity/string theory will likely provide additional sources for perturbations or gravitational potential independent of the primordial spectrum since they could contain more degrees of freedom. Therefore the TL correlation would reflect this input of new physical degrees of freedom by predicting a correlation different from one and with unique features on it which are used to identify the model.

We follow the approach of [14] in calculating the cross-correlation fluctuations C_l^{TL} between shear and temperature. Figure 3 shows our results for this cross correlation. In the figure, we take $b = 4.0 \times 10^9$ and 3.6×10^9 GeV as an example. Other parameters are taken as $\lambda = 0.1$ and $V_0 = 1.2 \times 10^{-8} M_{\rm P}^4$. The fact that our modification of the Friedmann equation comes as it does, i.e. from entanglement effects between our horizon patch and others, gives rise to some interesting and potentially unique features which we display in Figs. 3 and 4.

At large scales (low multipoles) we can see that the cross correlation of our model has essentially the same shape what would come from a LCDM model but with a suppressed amplitude. The reason for this is that, at those scales near the onset of inflation, the correction cutoff scale $\sigma(b, k)$ [which is obtained by substituting Eq. (2.7) into the definition of $\sigma(b, \phi)$] is nearly a constant and the overall

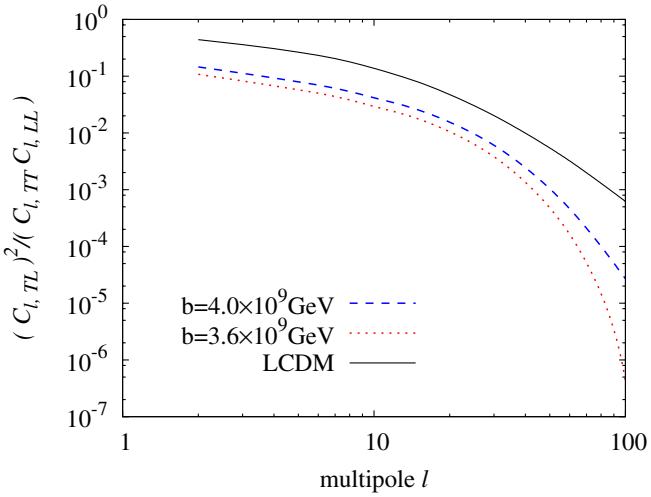

FIG. 3 (color online). Cross correlation between lensing and temperature are plotted. We assumed $b = 4.0 \times 10^9$ GeV (dashed line) and 3.6×10^9 GeV (dotted line) in this figure. For comparison, the case with ΛCDM (solid line) is also plotted.

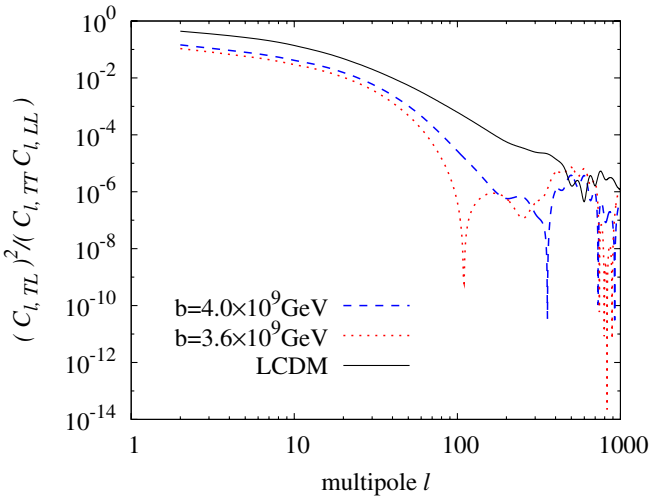

FIG. 4 (color online). The same as Fig. 3 except we plotted the larger range of multipoles here.

effect of its negative energy contribution is to slightly suppress the TT spectrum, Fig. 3. The most interesting and distinct features can be found at shorter scales $180 < l < 700$ as shown in Fig. 4. We see that around $l \simeq 200$ the correlation C_l^{TL} dips by about 3 orders of magnitude, with a ringing effect at structure formation scales and another dip in power at substructure scale, with ringing in between. The damping of this correlation means that much of the contribution to LSS is not coming from the primordial inflationary channel at those scales but from the correction term to the Newtonian potential given by $\sigma(b, k)$. We believe that these features correspond to the discontinuity found in the spectral index at around $k = 20$, $k = 40$ which arises from the changing in the dynamics of $\sigma(b, k)$. The ringing between them comes from Fourier transforming the two sharp features in k space into l space. These dips and ringing at structure scales are a result of the enhancement of power at these scales originating from the channel of the nonlocal entanglement. As we discussed above, the first one near $l \simeq 180$ may be correlated to the void appearing at the same scale, while the second damping originates from the potential modification term switching from negative to positive thereby going through a discontinuity at around $k = 40$, Fig. 4. These features may be distinguishable by future surveys.

IV. A SMOKING GUN FOR THE LANDSCAPE?

Much of the current discussion about string theory is centered around the question of whether any theory with a landscape of vacua as well populated as that of string theory could ever be predictive. Perhaps all we can do is look for correlations between various observables in each of the vacua of the landscape and make a very restricted set of ''predictions'' from these correlations. This is a rather bleak view of the future of physics, and one we do not share.

What we have shown in this work as well as its prequel is that, while we freely admit that the detailed behavior of the string landscape is still unknown, it is not out of the realm of possibility that we might be able to detect ''smoking-gun'' effects from it on the sky. In particular, the effects of the dynamics of quantum gravity, and, in particular, those due to nonlocal entanglements between our horizon patch and others, could modify the Friedmann equation and hence other cosmological observables and these modifications could be amenable to present or near future observations.

Let us summarize our results in more detail.

In paper I [5], we showed that the requirement of having a sufficiently flat inflationary potential *after* the modifications to the Friedmann equation are taken into account, coupled with the known value of the CMB quadrupole placed stringent bounds on the energy scale related to the structure of vacua in the non-SUSY part of the landscape. In our picture, this is the SUSY breaking scale, and we find that it has to be significantly larger (five to 8 orders of magnitude larger) than studies of the hierarchy problem would have required. The LHC will be able to test this statement soon, once again showing the tight interconnectivity between particle physics and cosmology.

Besides the tight bound on SUSY breaking scale, we find many interesting and perhaps unique clues imprinted on the CMB and on the large scale structure.

We have shown here how the negative, scale-dependent, energy correction in the modified Friedmann equation suppresses the temperature anisotropy spectrum at large angles, Fig. 1, which could help explain the observed suppression of power in the TT-spectrum by WMAP and COBE. The second and the third peak seems to also be mildly sensitive to the SUSY breaking scale b and to the scale of the nonlocal entanglement L_1. As we have explained in the text, this is related to the enhancement of power, Fig. 2, at structure and substructure scales and the scale-dependent modifications to the background Newtonian potential given by Eq. (3.4) which act as a source for the TT-spectrum.

The matter power spectrum is given in Fig. 2 and the modulation at scales after the last scattering shows up there too, although it is a small effect. However, as can be seen from Fig. 2, there are definite imprints on $P(k)$ with their origin in the corrections to the Newtonian potential coming from the quantum gravitational entanglement. The correction to the background Newtonian potential coming from the entanglement of our universe with superhorizon fluctuations of our inflaton patch and others leaves a definite imprint by damping structure at large scales and enhancing it at structure and substructure scales. As far as the linear theory is concerned, these corrections bring the matter power spectrum into much better agreement than LCDM with the data from the recent result of SDSS [11]. This also suggests that it may have implications for nonlinear modeling.

The effects we find here also provide a natural mechanism for creating primordial voids only at relevant scales $k \simeq 1$ and $k \simeq 20$. These effects come from the potential correction of the non-Gaussian nonadiabatic superhorizon fluctuations being superimposed on the background potential of the Gaussian perturbations thereby giving rise to a negative density contrast $\delta_f < 0$ at certain scales discussed above. The implications of this superimposition are twofold: It induces a running in the scalar spectral index n_s as calculated above, $n_s = n_s^0 + \delta n_s$, which is in agreement with the WMAP data [7], and it creates voids at large scales where the background and correction terms are comparable.

We showed in paper I [5] that the anisotropy scale contributing to the spectrum is bound to be at least 100 times greater than the horizon radius, namely $10^{-10}M_P < b < 10^{-8}M_P$, corresponding to roughly the first 1–10 e-foldings for GUT inflation. In terms of energies this stretches to about 18 e-foldings. This corresponds to primordial voids being created at $k \simeq 1$ or 50–60 degrees (causally disconnected part), in the sky or roughly at $l < 10$. Following the calculation done by Inoue and Silk [13] at the present epoch, the angle θ is given by the ratio of the size r_v to the distance d: $\sin\theta \simeq w = ar_v/d$. Their estimate shows that, for voids with $w \simeq 0.9$, $r_v \simeq r_H/10$ they agree with the SDSS findings of the observed two cold spots in the sky. As we have shown here the first voids are formed at $k \simeq 1$, $\theta \simeq 60$ which is in agreement with the SDSS findings. Thus, the void-induced quadruple suppression may explain the two observed cold spots since $\Delta T/T \simeq \delta\Phi/\Phi$.

The anticorrelation between the negative and positive density contrasts at low l ($l < 10$) shows itself as an alignment between the quadruple/octupole with more power concentrated along this direction [15,16] as shown in [13], i.e. a preferred direction along the correlation where the angular momentum dispersion is a maximum. The preferred direction is the line parallel to the vector connecting the centers of the voids located at 60 degrees. The superhorizon potential fluctuation related to the quadrupole scale acts as a gradient field with the quadrupole direction as the preferred axis. A more careful treatment of this issue requires a more detailed calculation of the evolution of the negative density contrasts, especially for the other voids located at $k = 20$, as well as the generation of the sky maps for this model. This is beyond the scope of this paper.

Our smoking gun which uniquely identifies the CMB and LSS signatures of this model, comes from cross correlating cosmic shear with temperature anisotropies. As discussed in [14], this cross correlation compares the sources that seed the lensing potential which maps large scale structure and the source that seeds CMB anisotropies. In the case of conventional inflation that source should be the primordial spectrum $P_{\mathcal{R}}$ and be the same for both CMB and LSS. Therefore a conventional cosmology predicts a correlation of order one. What we find here instead is that only the correlation is not close to 1, see Fig. 4, thereby demonstrating the existence of noninflationary channels contributing to structure, but that there are unique and rather interesting features in this spectrum at structure and substructure scales which soon will be observed by the PLANCK mission. This unique features come from the highly nontrivial expression of the nonlocal entanglement contained in $F(b, V)$, L_1. We can describe it physically by noting that the discontinuities induced on the scalar spectral index n_s show as the dips in Fig. 4. When Fourier transformed from k space to l-space, these together with the scale-dependent corrections on the Newtonian potential $\delta_f = \delta\Phi/\Phi^0$ show as ringing in the correlation for scales shorter after the surface of the last scattering. These are clearly very definite signatures that can be looked for by future surveys.

The main lesson to be taken from this, admittedly speculative, treatment of the dynamics of the landscape is that there are concrete calculations that can be done and concrete predictions that can be made. We addressed in Sec. IV how these highly nonlocal signatures of our Hubble patch with others can be distinguished from simple single field inflaton potentials. We would like to emphasize here that, as we have shown in both papers, the role of the landscape as the phase space for the initial patches is crucial in giving rise to the nonlocal entanglement of our Hubble patch with others originating from the initial mixing of our wave packet with other modes. The correction term in the Friedmann equations (2.2) and (2.3) derived from tracing out this highly nonlocal mixing (contained in the entanglement of the two parameters b with V) does not allow any freedom for changing its shape or parameters phenomenologically in order to fit the data thus providing a clear prediction for the model. We certainly do not argue that our results are *exactly* how the landscape behaves. Rather, there are interesting possibilities that may be robust enough to survive a more detailed analysis of the landscape. When a more detailed theory of the quantum gravity in the early universe is known, as we have demonstrated here, its astrophysical imprints may be within reach of observation in the cosmological arena.

ACKNOWLEDGMENTS

L. M-H. would like to thank K. Land and J. Magueijo for their help with voids. L. M-H. was supported in part by DOE Grant No. DE-FG02-06ER1418 and NSF Grant No. PHY-0553312. T. T. thanks K. T. Inoue for useful discussion. R. H. was supported in part by DOE Grant No. DE-FG03-91-ER40682. He would also like to thank the Perimeter Institute for their generous hospitality while this work was in progress.

[1] R. Holman and L. Mersini-Houghton, Phys. Rev. D **74**, 123510 (2006).
[2] R. Holman and L. Mersini-Houghton, arXiv/hep-th0512070 [Class. Quantum Gravity (unpublished)].
[3] A. Kobakhidze and L. Mersini-Houghton, Eur. Phys. J. C **49**, 869 (2007).
[4] L. Mersini-Houghton, Classical Quantum Gravity **22**, 3481 (2005); Jeffrey Crelinsten, *Einstein's Jury: The Race to Test Relativity* (Princeton University Press, Princeton, NJ, 2006); AIP Conf. Proc. **861**, 973 (2006); **878**, 315 (2006).
[5] R. Holman, L. Mersini-Houghton, and T. Takahashi, previous paper, Phys. Rev. D **77**, 063510 (2008).
[6] C. L. Bennett *et al.*, Astrophys. J. **436**, 423 (1994).
[7] Spergel *et al.*, Astrophys. J. Suppl. Ser. **170**, 377 (2007); http://lambda.gsfc.nasa.gov/product/map (2006).
[8] Mar Bastero-Gil, Katherine Freese, and Laura Mersini-Houghton, Phys. Rev. D **68**, 123514 (2003).
[9] F. Lucchin and S. Matarrese, Phys. Rev. D **32**, 1316 (1985).
[10] U. Seljak and M. Zaldarriaga, Astrophys. J. **469**, 437 (1996).
[11] M. Tegmark *et al.*, Phys. Rev. D **74**, 123507 (2006).
[12] C. R. Contaldi, M. Peloso, L. Kofman, and A. Linde, J. Cosmol. Astropart. Phys. 07 (2003) 002.
[13] K. T. Inoue and J. Silk, Astrophys. J. **648**, 23 (2006).
[14] S. Hannestad and L. Mersini-Houghton, Phys. Rev. D **71**, 123504 (2005).
[15] K. Land and J. Magueijo, Phys. Rev. Lett. **95**, 071301 (2005).
[16] M. Tegmark, A. de Oliveira-Costa, and A. Hamilton, Phys. Rev. D **68**, 123523 (2003); A. de Oliveira-Costa, M. Tegmark, M. Zaldarriaga, and A. Hamilton, Phys. Rev. D **69**, 063516 (2004).